Research Square

Preprints are preliminary reports that have not undergone peer review.
They should not be considered conclusive, used to inform clinical practice,
or referenced by the media as validated information.

Material characterization and thickness measurement of iron particle reinforced polyurethane multi-layer coating for aircraft stealth applications using THz-Time Domain Spectroscopy

A. Mercy Latha (mercy@ceeri.res.in)
CSIR-Central Electronics Engineering Research Institute (CEERI)
Sreedhar Unnikrishnakurup
A*STAR
Abhinandan Jain
DRDO
M. K. Pathra
DRDO
Krishnan Balasubramaniam
Indian Institute of Technology Madras

Research Article

Keywords: radar absorbing paint, terahertz, multi-layer coating, thickness measurement

Posted Date: April 21st, 2022

DOI: https://doi.org/10.21203/rs.3.rs-1559025/v1

License: This work is licensed under a Creative Commons Attribution 4.0 International License.
Read Full License

Material characterization and thickness measurement of iron particle reinforced polyurethane multi-layer coating for aircraft stealth applications using THz-Time Domain Spectroscopy

*A. Mercy Latha[1], Sreedhar Unnikrishnakurup[2], Abhinandan Jain[3], M. K. Pathra[3], Krishnan Balasubramaniam[4]

[1] *CSIR-Central Electronics Engineering Research Institute (CEERI), Chennai, India*

[2] *Institute of Material Research and Engineering (IMRE), A*STAR, Singapore*

[3] *Defense Laboratory Jodhpur, DRDO, Jodhpur, India*

[4] *Center for Nondestructive Evaluation, Indian Institute of Technology Madras, Chennai, India*

mercy@ceeri.res.in

Abstract

Particle reinforced polymer matrix composites (PMC) are widely used in the military aviation industry as a stealth coating for incident radar attenuation. These coatings are made up of many layers of different materials with varying thicknesses. In this study, we used terahertz (THz) spectral range by means of time-domain spectroscopy (TDS) to examine the thickness of iron particle reinforced polyurethane Radar Absorbing Paint (FE-PU-RAP) composite coatings non-destructively. For accurate estimation of the individual layer thickness in multi-layer coatings, precise knowledge of the material properties of the individual layers is a prerequisite. Hence, standalone samples of the individual layers have been initially employed to extract the material properties, such as the refractive index, absorption coefficient, etc. Then, the accurate thickness estimation by the time-of-flight measurement principle has been carried out using the reflected THz pulses. Further, since the individual reflected pulses from the multi-layered sample are overlapping in nature due to the optically thin coating thickness, a sparse deconvolution technique has been utilized for extracting each individual reflected time instant. The scattering from the iron particles also provides a challenge to the identification of the interface signals. This was addressed by optimizing the regularization parameter in the sparse deconvolution algorithm. With this technique, accurate estimation of each of the individual layers in the multi-layer sample has been accomplished, otherwise difficult non-destructively.

Keywords: radar absorbing paint, terahertz, multi-layer coating, thickness measurement

1 Introduction

For stealth requirements, particularly for aircrafts, the radar signature remain concealed from opponent electromagnetic spectrum sensors. A stealthy aircraft will be less visible (or, ideally, undetectable) to different detection equipment such as radar, laser, infrared (IR), visual, near-infrared (NIR), or sonic sensors [1]. Stealth technology strives to lower radar cross-section (RCS) by appropriate geometric design and/or the use of radar-absorbing materials and structures. The first radar-absorbing substance created artificially was ferrite-based paint [2]. Radar Absorbing Materials (RAMs) are also commonly used for electromagnetic (EM) radiation protection from high-intensity radiated fields, natural phenomena (lightning), intentional EM interference, and nuclear EM pulses, as components of shields used in particle accelerators, for EM compatibility issues (equipment level shielding, anechoic chambers testing), and for human exposure mitigation. By including EM conductive fillers into the bulk matrix, composite-based multi-layered structures can create effective graded RAM [3]. Polymer Matrix Composites (PMCs) are widely employed as radar absorbent structures (RAS) due to their excellent radar absorption capabilities and structural performance [4]. Thickness inspection of these PMCs is necessary both during the layer-by-layer spray fabrication of the RAP and at regular intervals to get the desired results. These coatings have airborne application and are subjected to severe stresses at speeds ranging from 1 to 2 Mach. This causes significant service degradation, such as cracking, erosion, and delamination from the substrate. This necessitates the use of an NDE technique to determine the coating thickness of specific layers that are only accessible from one side.

Terahertz (THz) waves ranging from 0.1 THz to 10 THz can penetrate through most non-metallic materials, thereby making identification/detection of internal details, within a non-metallic object, possible [5] -[6]. This property has enabled THz waves to be successfully employed in various non-metallic nondestructive testing (NDT) applications, such as ceramic matrix composite materials (CMC) [7], GFRP [8], and thermal barrier coating [9]. Since THz-based NDT doesn't demand a coupling medium and proximity as required by ultrasonic NDT, this technique is non-contact and non-invasive. Further, the photon energy levels of the THz radiation are very less, and it is non-ionizing in nature as opposed to many other methods viz. X-rays[10]. THz-NDT can probe deeper into the dielectric material in evaluating the sub-surface and bulk defects compared to infrared thermographic techniques.

In THz-NDT, THz pulsed time-domain spectroscopy (TDS) is the widely used technique wherein the transmitted or reflected characteristics of a THz picosecond pulse are studied through the sample[11]. From the pulse characteristics, valuable information regarding the material parameters or thickness information can be ascertained. The time-of-flight (TOF) technique has been traditionally adopted for thickness estimation, wherein the time delays between the reflected pulses from different interfaces are measured. From the measured time delays and knowledge of the refractive index, the thickness of the individual layers can be estimated precisely [12].

Direct time-of-flight methodology fails under the following circumstances:

1) when temporal THz echoes reflected from various interfaces overlap, particularly when the specimen is optically very thin [13];

2) when temporal THz echoes reflected from low reflection interfaces are of the order of the noise floor, particularly when the refractive index between layers are not very different;

3) when the pulse width of the reflected temporal THz echo gets spread due to THz wave scattering from sub-wavelength particles [14].

These particular scenarios demand advanced signal processing techniques to restore the reflected echoes from each sample interface for stratigraphic evaluation.

Deconvolution techniques are utilized to extract the sample impulse response function, which contains sharp peaks, corresponding to the reflection from various interfaces of the sample. The conventional deconvolution approach provides the required impulse response of the sample by calculating the inverse Fourier transform of the transfer function (ratio of reflected and incident spectrum) While this is a straight-forward approach,this operation introduces severe ringing effects and high amplitude spikes in the high-frequency range. These artifacts are not desirable. Hence, an alternative technique, namely frequency-wavelet deconvolution techniques, has been employed [15].

In the frequency-wavelet deconvolution technique, frequency-domain filtering is carried out, followed by wavelet denoising. Several frequency-domain filters, namely double Gaussian [16], Wiener [17], tapered cosine apodization [18], Hanning window, or von Hann filter [19], have also been explored by various researchers to improve the performance of this technique. However, the depth resolution of this technique is greatly dependent on the frequency-domain filter parameters.

Hence, an alternate technique, namely sparse deconvolution utilizing the sparsity of the impulse response function, has been employed. Previous literature [20] reveals the application of sparse deconvolution technique along with iterative shrinkage algorithm to estimate the thickness of mill-scale ~5 μm. In this work, the sparse deconvolution technique has been employed to quantitatively characterize the layer thicknesses of each layer in a multi-layered RAP sample.

Additional complexity has been imposed due to an intermediate coating layer in the RAP which is impregnated with iron particles. The scattering from the iron particles was manifesting as reflections in the as-received THz signals from the multi-layered structure. These reflections were overlapping with the interface signals and also contributed to the challenge of identifying the different interface echos. This difficulty was addressed by optimizing the regularization parameter in the sparse deconvolution technique.

2 Materials and Methods

2.1 FE-PU-RAP Composite Multi-layer coating system

The FE-PU-RAP consists of two component polyurethane (PU) as resin and iron metal flakes as filler material. The paint is manufactured by mixing the ingredients in a bead mill for homogeneous dispersion. The prepared paint is then applied by conventional spray method on a primer coated metal or fiber reinforced polymer substrate. Figure 1 (a) shows the composites with polyurethane resin reinforced with randomly distributed iron micro-particles. The thickness of the metal substrate is 1 mm, the primer coating on top of the substrate ranges from 70-80 µm, the iron particle reinforced polyeurethane (FE-PU) coating thickness is 1.6 ± 0.1mm and the PU top coat is 80-100 µm. Figure 1(b) shows iron particle dispersion in the PU resin in a slice of the CT scan of the FE-PU layer. The white specks are iron particles scattered throughout the gray PU resin, while the black dots are pores.

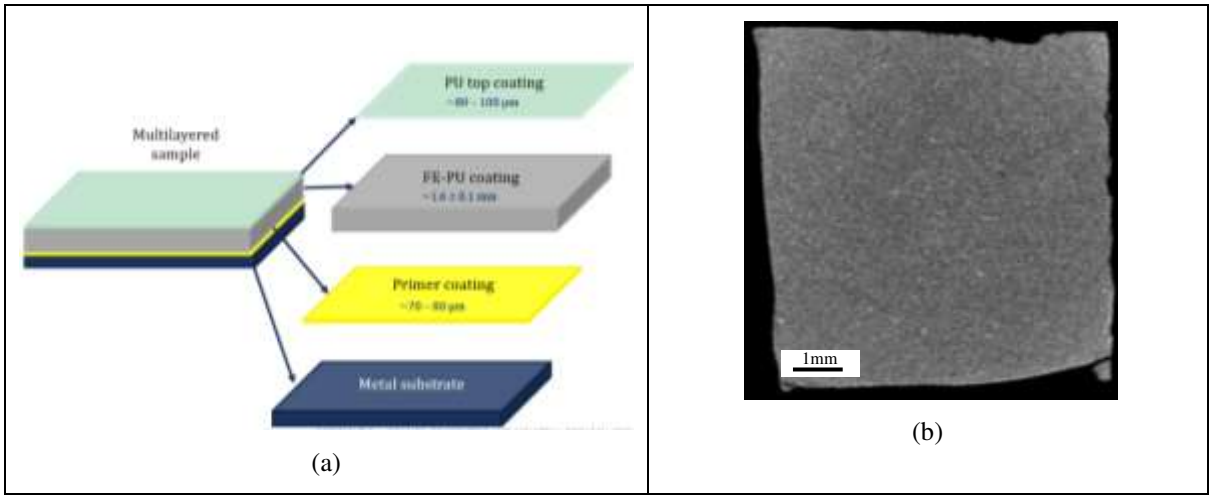

Figure 1(a)Schematic diagram of the arrangement of the multi-layered FE-PU-RAP sample (b) CT slice of the FE-PU composite layer.

2.2 Material Characterization-

The individual coating layer thickness can be estimated accurately with prior knowledge of the optical material properties of each layer in terms of refractive index. However, the refractive indices of these materials are not readily available in the literature. Hence, precise extraction of the refractive index of each layer is required, which demands standalone samples for each layer.

Standalone samples of PU top and FE-PU layers have been synthesized with a thickness of 0.5 mm and 1.8 mm, respectively. These standalone samples have been used in the THz pulsed TDS system to acquire the THz transmission coefficient of the sample for the frequencies ranging from 0.1 to 2 THz. The material parameters are extracted from the measured transmission coefficient values using the following approach proposed by [21].

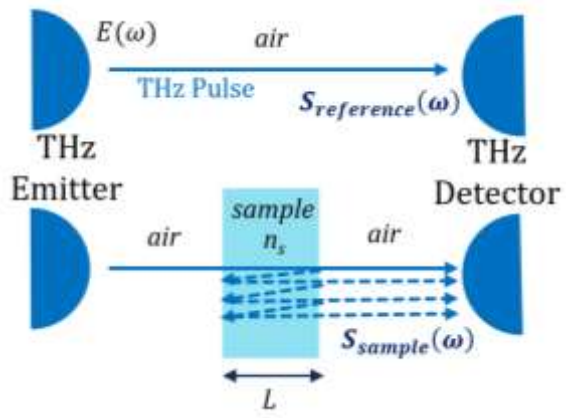

Figure 2 Schematic diagram of the THz pulse transmission in air and sample

The transmitted THz electric field without the sample, as in Figure 2, has the following spectral component:

$$S_{reference}(\omega) = \eta(\omega).P_{air}(\omega, L)\,.E(\omega) \quad \ldots (1)$$

where $P_{air}(\omega, L)$ is the propagation coefficient of THz pulse in air

The spectral component of transmitted THz electric field through the sample, as in Figure 2, is as follows:

$$S_{sample}(\omega) = \eta(\omega).T_{as}(\omega).P_s(\omega, L).T_{sa}(\omega).\sum_{k=0}^{+\infty}\{R_{sa}(\omega).P_s^2(\omega, L).R_{as}(\omega)\}^k.E(\omega) \quad \ldots (2)$$

Where the $T_{as}(\omega)$ and $R_{as}(\omega)$ are the transmission and reflection coefficients from the air to sample medium with refractive index n_s, respectively. And, $P_s(\omega,d)$ is the propagation coefficient in the sample. These coefficients are defined as follows:

$$T_{sa}(\omega) = \frac{2}{\tilde{n}_s + 1} \quad \ldots (3)$$

$$R_{sa}(\omega) = \frac{\tilde{n}_s - 1}{\tilde{n}_s + 1} \quad \ldots (4)$$

$$P_s(\omega, L) = exp\left[-i\frac{\tilde{n}_s\omega L}{c}\right] \quad \ldots (5)$$

$$P_{air}(\omega, L) = exp\left[-i\frac{\omega L}{c}\right] \quad \ldots (6)$$

The theoretical complex transmission coefficient is thus obtained as

$$T_{theoretical}(\omega) = \frac{S_{sample}(\omega)}{S_{reference}(\omega)} = \frac{4\tilde{n}_s}{(\tilde{n}_s + 1)^2} exp\left[-i\frac{(\tilde{n}_s - 1)\omega L}{c}\right].FP(\omega) \quad \ldots (7)$$

where

$$FP(\omega) = \left[1 - \left(\frac{\tilde{n}_s - 1}{\tilde{n}_s + 1}\right)^2 .exp\left[-2i\frac{\tilde{n}_s\omega L}{c}\right]\right]^{-1} \quad \ldots (8)$$

The measured transmission coefficient is obtained by taking the ratio of the measured sample spectrum to the measured reference spectrum. The complex refractive index value is computed by minimizing the error function, which is the difference between the theoretical and measured complex transmission coefficient as $T_{theoretical}(\omega) - T_{measured}(\omega)$. However, this error function is oscillating, and hence the error function has been modified [21] as

$$\Delta_{modified}(\tilde{n}_s) = (ln(|T_{theoretical}(\omega)|) - ln(|T_{measured}(\omega)|))^2 + \left(arg\left(T_{theoretical}(\omega)\right) - arg(T_{measured}(\omega))\right)^2 \quad \ldots (9)$$

The modified error function $\Delta_{modified}$ as in equation (9), is smooth, monotonous, and parabolic, which results in faster convergence to the minimum. The above-mentioned approach has been used for the material parameter extraction of standalone samples of the PU top layer and FE-PU layers.

A standalone sample could not be synthesized for the primer layer, so a bilayer sample with primer and FE-PU layer has been provided. This bilayer sample has been used in transmission mode, and an advanced extraction algorithm, as explained by [22] has been used for the material parameter extraction.

2.3 Thickness Estimation

For thickness estimation, the pulsed THz-TDS system is employed in the reflection setup, as shown in Figure 3. The incident THz pulse is first recorded by collecting the reflected pulse from a perfect reflector. Then, the THz pulse is illuminated on the coated sample, from which the reflected pulse is detected, which is time-delayed and attenuated. The time delay is the propagation time of the THz pulse within the coating material before its reflection from the substrate, which is proportional to the refractive index of the coating material.

$$\Delta t = \frac{2d}{c/n} \qquad \ldots(10)$$

where Δt is the time delay between the incident and reflected pulses, d is the coating thickness, c is the velocity of light, and n is the refractive index of the coating material. The coating thickness can be obtained by rearranging equation (10) from the estimated time delay value with the prior knowledge of the refractive index value.

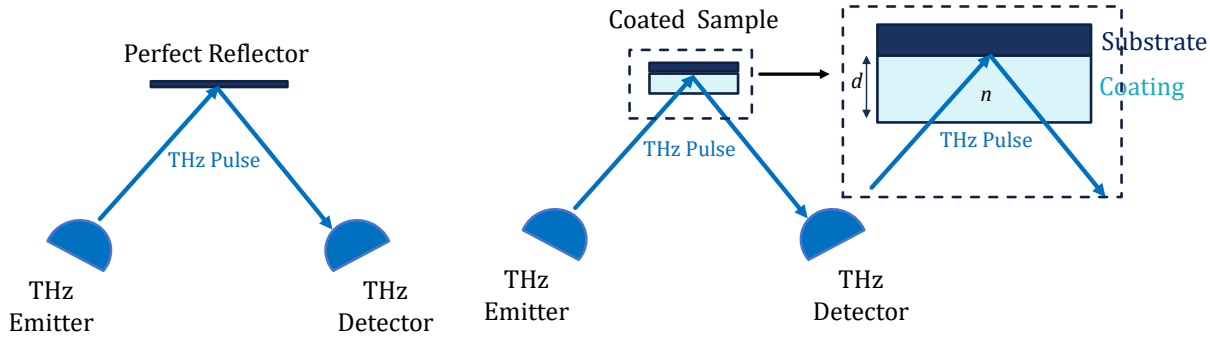

Figure 3 Schematic diagram of the THz pulse reflected from the perfect reflector and coated sample

3 THz experimental setup

3.1 THz transmission experiments for material characterization

As mentioned in section 2.2, the material parameter extraction studies are performed with the standalone samples in the transmission mode, as shown in Figure 4. In the transmission setup, the sample is placed in the transmission path of the THz beam. The pulsed THz beam is generated by a bowtie photoconductive antenna where a photoconductive gap exists between the electrodes across which an electrical bias is applied. The photoconductive gap is illuminated by an ultra-fast femtosecond laser pulse of pulse width 80 fs and repetition frequency of 100 MHz. When the femtosecond pulse is exposed to the photoconductive gap, the conductivity of the photoconductive material increases significantly, causing current flow across the electrodes. The photo-generated transient current results in the radiation of a sub-picosecond THz pulse. The radiated THz pulse is divergent in nature, and hence a pair of plano-convex lenses are used to focus the beam to a point on the sample. The transmitted pulse from the sample is correspondingly collected by a photoconductive receiver antenna, which works on the reverse of the principle mentioned above. A current proportional to the strength of the incident THz pulse is generated in the receiver PCA and detected using a lock-in amplifier.

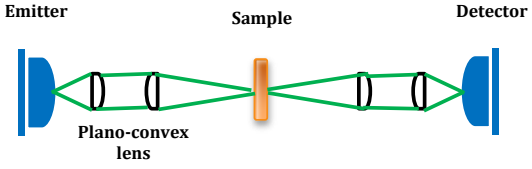

(a)

(b)

Figure 4 THz-TDS experimental setup in transmission mode (a) Scchematic diagram (b) Photograph of sdexperimental setup

Initially, the incident THz pulse (reference pulse) is recorded without the sample for a time window of 40 ps. Then, the sample is placed at the focal point of the focusing lens, and the corresponding transmitted pulse through the sample is recorded for the same duration of the time window, which is shown in the figure 4.

3.2 THz reflection experiments for thickness measurements

For the thickness estimation, the THz TDS system is employed in reflection mode, as shown in Figure 5. The THz pulse from the photoconductive antenna is focussed on the sample, and the reflected pulse is collected by the photoconductive receiver antenna through two pairs of the plano-convex lens. The reflected THz pulse contains the echoes from each interface based on the respective Fresnel's reflection coefficient arising due to the difference of refractive indices. The thickness of each layer can be estimated by computing the time delay between the echoes of the interfaces with the knowledge of the refractive index of the layer. But, if the layers are optically thin (optical distance between the interfaces are higher than the pulse width of the THz pulse), the reflected echoes would be over-lapping and computation of the time delay is not straightforward, which demands advanced signal processing techniques to be employed.

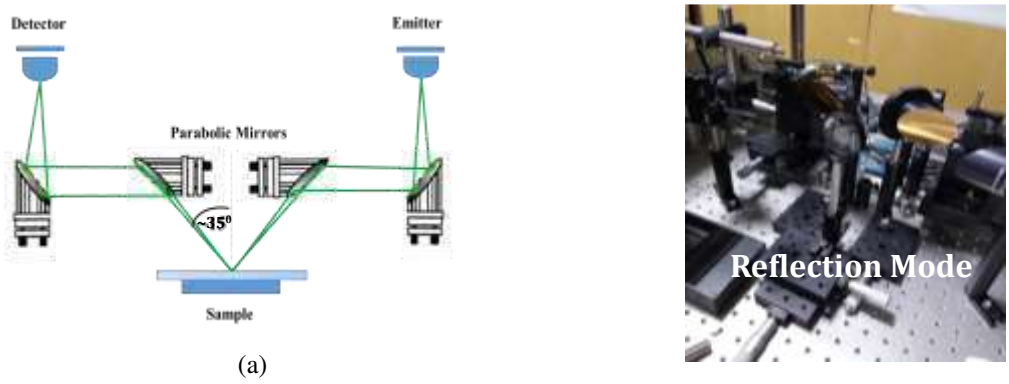

(a) (b)

Figure 5 THz-TDS experimental setup in reflection mode (a) Schematic (b) photographof the reflection measurement

4 THz measurement results

As previously mentioned, material parameter extraction of the standalone samples of PU top and FE-PU samples has been performed using the pulsed THz-TDS system in transmission mode. In Figure 6, the incident THz pulse is depicted in red color, and the transmitted THz pulse through the sample is shown in blue color. It could be observed that the transmitted pulse is time-shifted due to the additional optical distance the pulse had to be travel before reaching the detector. Further, the pulse is of lesser amplitude than the incident pulse accounting for the absorption loss in the sample.

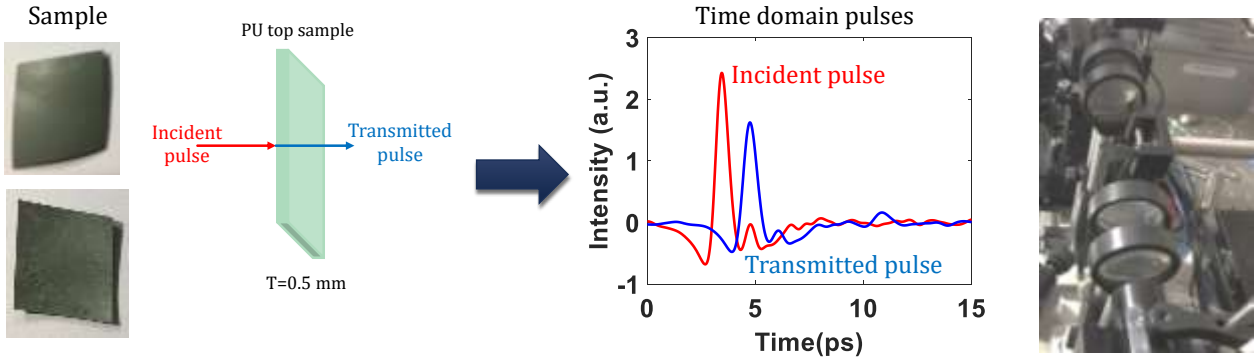

Figure 6 THz-TDS measurement results for the standalone sample of PU-top layer

A similar trend of time-shifting and reduced amplitude pulse has been observed for the FE-PU sample, as shown in Figure 7. However, the peak-to-peak amplitude of the transmitted pulse is of the order of ~0.125 a.u. (which is reduced by > 95% compared to the incident pulse). The amplitude reduction could be attributed to the high THz

absorption coefficient of the standalone FE-PU layer contributed by the increased thickness and the iron particles reinforcement inside the sample.

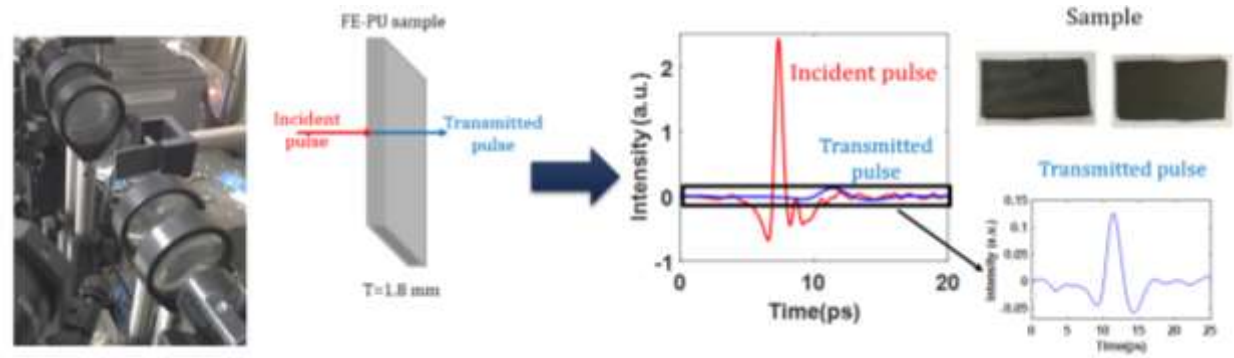

Figure 7 THz-TDS measurement results for the standalone sample of FE-PU layer

The refractive index and absorption coefficient extracted for the PU-top and FE-PU layers based on the minimization approach mentioned in the previous section is shown in Figure 8 (a) and (b), respectively.

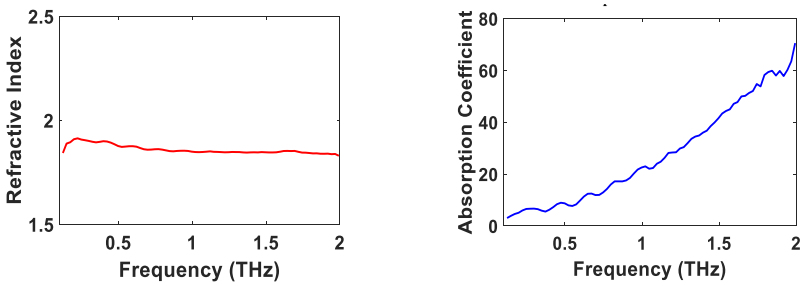

(a)

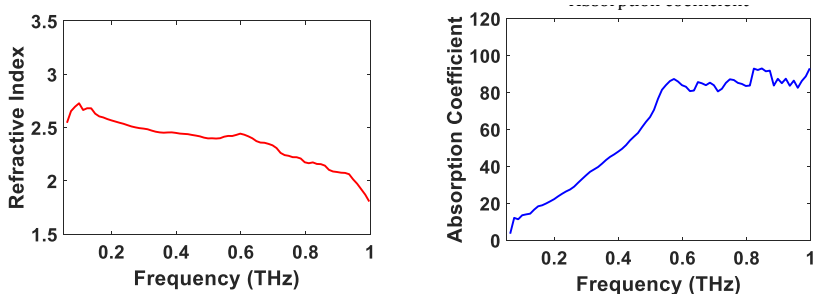

(b)

Figure 8 Extracted material parameters of the (a) PU-top and (b) FE-PU-RAP layer

For extraction of the material properties of the primer layer, a bilayer sample of FE-PU and primer has been used. The incident and transmitted pulse through the bilayer sample are shown in Figure 9, which is similar to the pulse through the FE-PU sample due to the higher thickness of the FE-PU layer compared to the primer layer. It could be observed that the amplitude of the reflected signal is very low which is due to the high THz absorption of the bilayer sample. The extracted material parameters of the bilayer sample are shown in Figure 10. From the figs, the average refractive indices of the three coatings are inferred and are presented in Table 1.

After the material parameter extraction of each individual layer, the multi-layered sample has been placed in a reflection setup, and the reflected pulse from the THz-TDS system has been recorded, which is shown in Figure 11. Clearly, from Figure 11, individual reflections are not visible in the reflected pulse (blue) and appear to be overlapped with each other. Hence, sparse deconvolution has been performed, whose results are depicted in Figure 12. Fig. 12 shows multiple peaks as opposed to the expected three peaks at the four interfaces ((1) air to PU-top interface, (2) PU-top to FE-PU interface, (3) FE-PU to primer interface, and (4) primer to the metal substrate interface). The extra peaks were observed within the FE-PU layers, which can be attributed to the iron particles

dispersed in the FE-PU layer. S-ince many peaks are available in the sample impulse response, identifying the right peaks has been done by optimization of the regularization parameter used in the sparse deconvolution algorithm. The regularization parameter plays an important role in hitting a compromise between the sparsity of the impulse response function and the residual norm. The time delay values estimated from the deconvolved results have been tabulated in the Table 2 for four different measurement points. These delay values have been used for computing the thickness of each individual layer, as in Table 2.

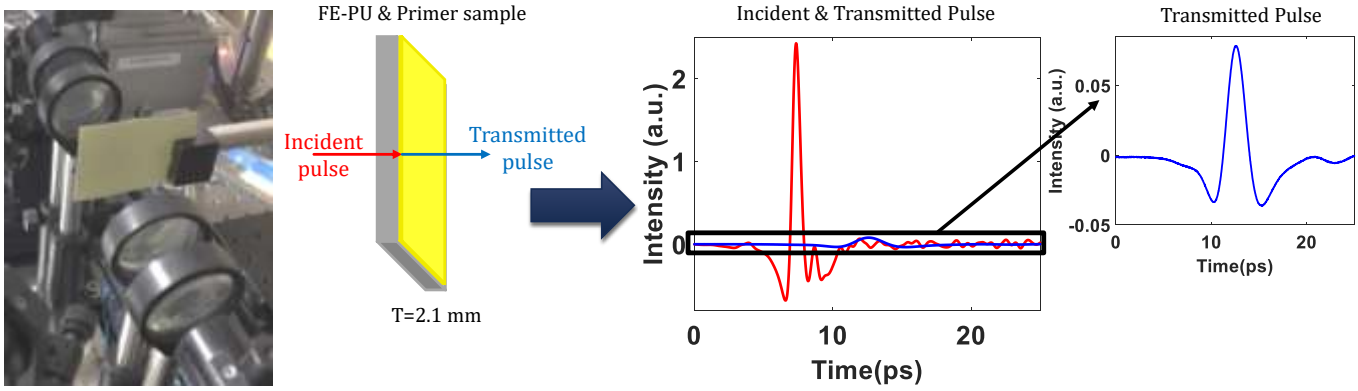

Figure 9 THz-TDS measurement results for the standalone sample of FE-PU and primer bilayer

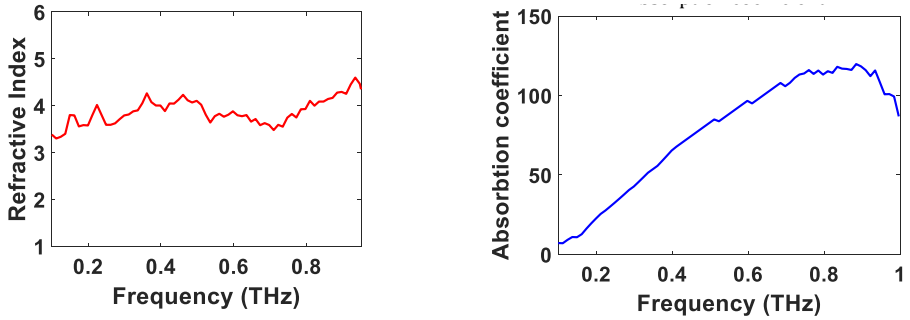

Figure 10 Extracted material parameters of the primer layer

Table 1 Averaged refractive indices of individual coatings

Material	Refractive Index
PU-top	1.86 ± 0.01
FE-PU-RAP	2.14 ± 0.03
Primer	3.94 ± 0.08

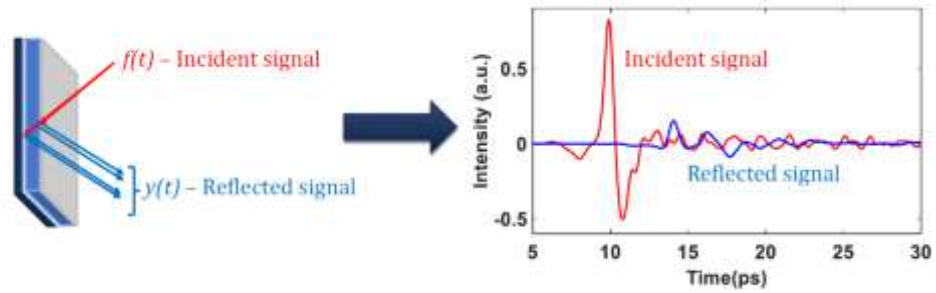

Figure 11 THz pulse incident and reflected from the multi-layered sample

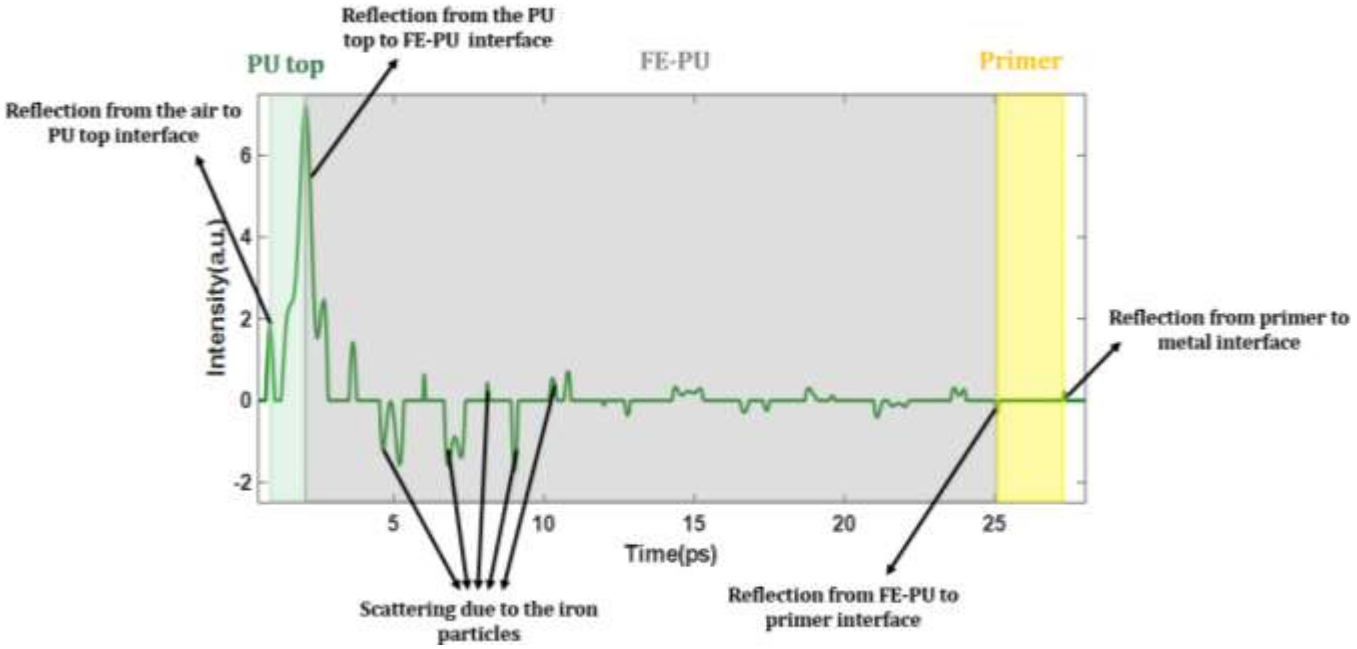

Figure 12 Results of sparse deconvolution showing various interfaces as distinct peaks

Table 2 Summary of the estimated delay and estimated thickness at each layer

Measurement point	Estimated delay (ps)	Estimated thickness (µm)	Average thickness (µm)
PU top layer (n=1.86)			
1	1.05	84.91	98.67
2	1.24	100.21	
3	1.26	102.21	
4	1.32	106.93	
FE-PU layer (n=2.13)			
1	23.40	1647.88	1638.96
2	22.93	1614.93	
3	23.41	1649.26	
4	23.34	1643.76	
Primer layer (n=3.94)			
1	2.32	88.45	72.28
2	2.02	77.30	
3	1.65	63.18	
4	1.57	60.20	

5 Conclusion

In this paper, the layer thicknesses of a multi-layered coating on a metal substrate have been demonstrated. One of the layers is populated with iron particles which exhibit both absorbing and scattering phenomena. To estimate the individual coating layer thickness in the FE-PU-RAP coating system, initially, the material parameter of each layer has been extracted using standalone samples. After precise extraction of the material parameters, the

reflected THz pulse from a multi-layered composite polyurethane sample was obtained, where the individual reflected echoes were found to be overlapping. Hence, to resolve each echo, a sparse deconvolution technique was employed, resulting in an accurate estimate of the thickness of each layer. The scattering effects from the iron particles was addressed by optimization of the regularization parameter in the sparse deconvolution algorithm. This approach of using THz-TDS measurements for determining the multi-layered coated metal substrate samples overcomes the limitations of other NDE methods for similar applications.

Declarations

Ethical Approval

Not applicable

Consent to Participate

Not applicable

Consent to Publish

Not applicable

Authors Contributions

A. Mercy Latha and Sreedhar Unnikrishnakurup wrote the main manuscript text and carried out the experimental studies. Abhinandan Jain and M. K. Pathra provided the coated samples and the technical inputs regarding the RAP coating and process. Krishnan Balasubramaniam supervised the research work and provided his constant guidance. And all authors reviewed the manuscript.

Funding

The authors have no relevant financial or non-financial interests to disclose.

Competing Interests

The authors declare that they have no competing interests as defined by Springer, or other interests that might be perceived to influence the results and/or discussion reported in this paper.

Availability of data and materials

Not applicable

6 Reference

[1] C. G. Jayalakshmi, A. Inamdar, A. Anand, and B. Kandasubramanian, “Polymer matrix composites as broadband radar absorbing structures for stealth aircrafts,” *J. Appl. Polym. Sci.*, vol. 136, no. 14, pp. 1–21, 2019, doi: 10.1002/app.47241.

[2] R. G. Sheffield, *The official F-19 stealth fighter handbook*. Compute! Books, 1989.

[3] Q. Liu, B. Cao, C. Feng, W. Zhang, S. Zhu, and D. Zhang, “High permittivity and microwave absorption of porous graphitic carbons encapsulating Fe nanoparticles,” *Compos. Sci. Technol.*, vol. 72, no. 13, pp. 1632–1636, 2012.

[4] N. Khatavkar and K. Balasubramanian, “Composite materials for supersonic aircraft radomes with ameliorated radio frequency transmission-a review,” *RSC Adv.*, vol. 6, no. 8, pp. 6709–6718, 2016.

[5] S. Zhong, “Progress in terahertz nondestructive testing: A review,” *Front. Mech. Eng.*, vol. 14, no. 3, pp. 273–281, 2019.

[6] I. Amenabar, F. Lopez, and A. Mendikute, “In introductory review to THz non-destructive testing of composite mater,” *J. Infrared, Millimeter, Terahertz Waves*, vol. 34, no. 2, pp. 152–169, 2013.

[7] J.-Y. Zhang, J.-J. Ren, L.-J. Li, J. Gu, and D.-D. Zhang, “THz imaging technique for nondestructive analysis of debonding defects in ceramic matrix composites based on multiple echoes and feature fusion,” *Opt. Express*, vol. 28, no. 14, pp. 19901–19915, 2020.

[8] K. H. Im, S. K. Kim, Y. T. Cho, Y. D. Woo, and C. P. Chiou, “Thz-tds techniques of thickness measurements in thin shim stock films and composite materials,” *Appl. Sci.*, vol. 11, no. 19, 2021, doi: 10.3390/app11198889.

[9] S. Unnikrishnakurup, J. Dash, S. Ray, B. Pesala, and K. Balasubramaniam, “Nondestructive evaluation of thermal barrier coating thickness degradation using pulsed IR thermography and THz-TDS measurements: A comparative study,” *NDT E Int.*, vol. 116, 2020, doi: 10.1016/j.ndteint.2020.102367.

[10] M. Bessou *et al.*, “Advantage of terahertz radiation versus X-ray to detect hidden organic materials in sealed vessels,” *Opt. Commun.*, vol. 285, no. 21–22, pp. 4175–4179, 2012.

[11] D. Wu, C. Haude, R. Burger, and O. Peters, “Application of terahertz time domain spectroscopy for NDT of oxide-oxide ceramic matrix composites,” *Infrared Phys. Technol.*, vol. 102, p. 102995, 2019.

[12] M. Zhai, A. Locquet, C. Roquelet, P. Alexandre, L. Daheron, and D. S. Citrin, “Nondestructive measurement of mill-scale thickness on steel by terahertz time-of-flight tomography,” *Surf. Coatings Technol.*, vol. 393, no. August 2019, p. 125765, 2020, doi: 10.1016/j.surfcoat.2020.125765.

[13] M. Zhai, A. Locquet, C. Roquelet, and D. S. Citrin, “Terahertz time-of-flight tomography beyond the axial resolution limit: autoregressive spectral estimation based on the modified covariance method,” *J. Infrared, Millimeter, Terahertz Waves*, vol. 41, no. 8, pp. 926–939, 2020.

[14] S. Zhou *et al.*, “Terahertz signal classification based on geometric algebra,” *IEEE Trans. Terahertz Sci. Technol.*, vol. 6, no. 6, pp. 793–802, 2016.

[15] G. C. Walker *et al.*, “Terahertz deconvolution,” *Opt. Express*, vol. 20, no. 25, pp. 27230–27241, 2012.

[16] Y. Chen, S. Huang, and E. Pickwell-MacPherson, “Frequency-wavelet domain deconvolution for terahertz reflection imaging and spectroscopy,” *Opt. Express*, vol. 18, no. 2, pp. 1177–1190, 2010.

[17] S. Ghael, A. M. Sayeed, and R. G. Baraniuk, “Improved wavelet denoising via empirical Wiener filtering,” in *SPIE Technical Conference on Wavelet Applications in Signal Processing*, 1997.

[18] R. K. H. Galvão, S. Hadjiloucas, A. Zafiropoulos, G. C. Walker, J. W. Bowen, and R. Dudley, “Optimization of apodization functions in terahertz transient spectrometry,” *Opt. Lett.*, vol. 32, no. 20, pp. 3008–3010, 2007.

[19] J. Dong, X. Wu, A. Locquet, and D. S. Citrin, “Terahertz superresolution stratigraphic characterization of multilayered structures using sparse deconvolution,” *IEEE Trans. Terahertz Sci. Technol.*, vol. 7, no. 3, pp. 260–267, 2017.

[20] M. Zhai, D. S. Citrin, and A. Locquet, “Terahertz Nondestructive Stratigraphic Analysis of Complex Layered Structures: Reconstruction Techniques,” *J. Infrared, Millimeter, Terahertz Waves*, vol. 42, no. 9, pp. 929–946, 2021.

[21] L. Duvillaret, F. Garet, and J.-L. Coutaz, “A reliable method for extraction of material parameters in terahertz time-domain spectroscopy,” *IEEE J. Sel. Top. quantum Electron.*, vol. 2, no. 3, pp. 739–746, 1996.

[22] B. Jin *et al.*, “Extraction of material parameters of a bi-layer structure using Terahertz time-domain spectroscopy,” *Sci. China Inf. Sci.*, vol. 57, no. 8, pp. 1–10, 2014.